

Process Optimization of Aerosol Based Printing of Polyimide for Capacitor Application

D. M. Keicher*, J. M. Lavin*, L. N. Appelhans*, S. R. Whetten*, M. Essien**, S. S. Mani*, P. B. Moore*, A. Cook*, N. A. Acree*, N. P. Young*, M. J. Russell*

*Sandia National Laboratories, 1515 Eubank SE, Albuquerque, NM 87123

**Castor Technologies, 61 Manana Dr. Cedar Crest, NM 87008

Abstract

Direct write printing approaches provide the opportunity for additive manufacturing (AM) to impact the electronics industry. This class of technologies provides a path to cost effectively print electronic components in low volume, high mix production. The printed electronics technologies provide an opportunity to explore new materials, new processing approaches and unique component configurations to alter the electronics industry. A new project underway to explore printing of planar, nonplanar and three-dimensional capacitors will be discussed. Aerosol based printing technologies applied to dielectric printing have demonstrated the ability to print small features in three dimensions. This presentation will cover recent research in optimizing process variables both with materials and deposition parameters to obtain desirable film properties. This work will compare the film properties using the additive manufacturing approach to traditional casting. Finally, this presentation will describe an optimized process in detail and the rationale for the processes chosen.

Introduction

The field of printed electronics (PE) provides the opportunity to radically change how macro electronic components are manufactured⁽¹⁻⁴⁾. Analogous to, yet less mature, than 3D printing of mechanical hardware, PE technologies offer significant benefit over traditional, large volume manufacturing techniques. An example of the type of benefit offered through the PE approach is shown graphically in Figure 1. This figure shows a typical process for applying and patterning a single material layer using a lithographic approach (Fig. 1 (left)) versus a PE approach (Fig. 1(right)). Several advantages are immediately evident from this comparison: (1) many of the very expensive capital equipment factory pieces can be eliminated, (2) tooling needs are also significantly reduced since the printers can be reconfigured digitally (i.e. product specific masks, hard tooling, etc.), (3) the digital manufacturing environment is highly configurable providing an agile manufacturing environment, (4) fewer process steps and (5) customizable for low volume/high mix production.

To advance the state of the art in printing of electronic components, a project has been initiated to explore opportunities for printing capacitors. Capacitors are widely used in most electronic circuits and yet the capacitor technology remains largely unchanged for many applications. The focus of this effort is to explore opportunities to apply PE technologies directly print capacitors. Two areas of exploration include: (1) printing capacitors onto non-traditional and non-planar surfaces and (2) to enhance the capacitance value by printing electrodes and dielectrics with 3D features with increased surface area. Previous work performed in semiconductor materials ^(5,6) have shown significant enhancement in capacitance density using etched and plated trench capacitors. These studies have shown enhancement in capacitance density of 16 fF/cm² and 9 fF/cm², respectively. This type of enhancement could radically enhance performance margins and lead to significant reduction in the size of equivalent components. Yet another related and significant area of exploration is to develop the ability to directly print capacitors (and other multi-material) components directly onto non-traditional and non-planar surfaces.

Initial work on this project focused on understanding how to apply dielectric films directly onto arbitrarily shaped surfaces. Several printing techniques have been explored and the results of the aerosol based printing will provide a focus for this article.

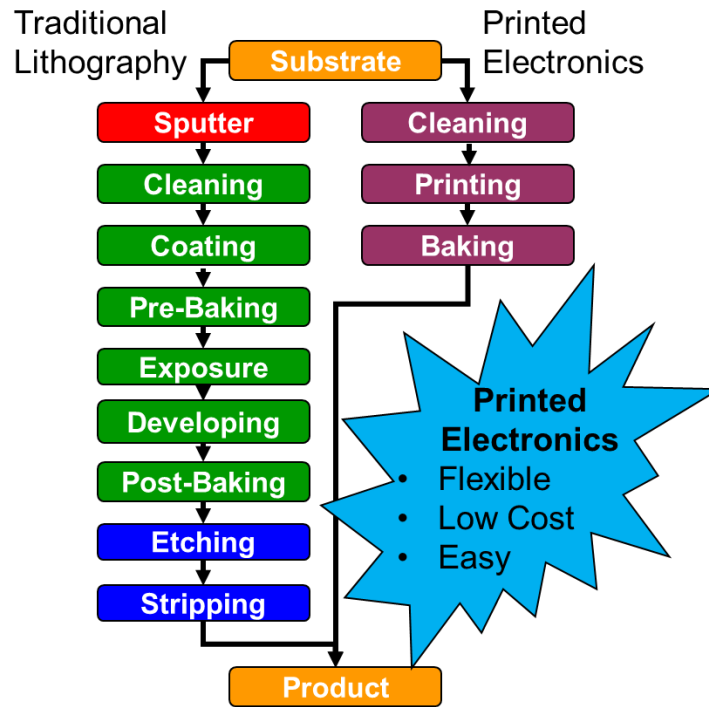


Figure 1. Graphical representation showing process steps for applying a single, patterned material layer using traditional lithography versus process steps for applying a single, patterned material layer using a printed electronics approach.

Experimental

To create uniform films on non-planar surfaces, it was necessary to identify/develop processes that would allow the film material to remain where it was deposited without flowing away from the deposition area. It was equally important that these films have very good dielectric properties providing good electrical break down strength. Two spray processes were investigated as methods to deposit the films using aerosol droplets from a polyimide solution. The first print technology used was a Sono-Tek Accumist (STA) spray head that has a resonant frequency of 38 kHz (see Figure 2a). The STA spray head generates droplets ranging in size from 30-40 μm . The STA head is capable of aerosolizing liquid materials ranging from one to a few hundred centipoise (cP). The fluid is fed to the deposition nozzle using a syringe pump and the volumetric federate of the fluid is controlled to ensure that constant spray output is achieved. A sheath gas is used to minimize spray column divergence and to accelerate the droplets to impact onto the print substrate. A heated platen is used to control the substrate temperature to affect the rate of solvent evaporation from the aerosol droplets and the printed polyimide film. The platen is attached to a computer numerical control (CNC) motion platform to print the film using specific motion pattern. An off the shelf CNC motion control system from FlashCut was used for motion control and to drive the syringe pump used to feed the STA nozzle. The printed linewidth from the STA spray head ranges from 1.78 mm to 25 mm. The output rate from the STA spray head can be varied from 1-100 mL/hr. Due to the ability to quickly coat large areas, most experimental work discussed was obtained using the STA nozzle technology.

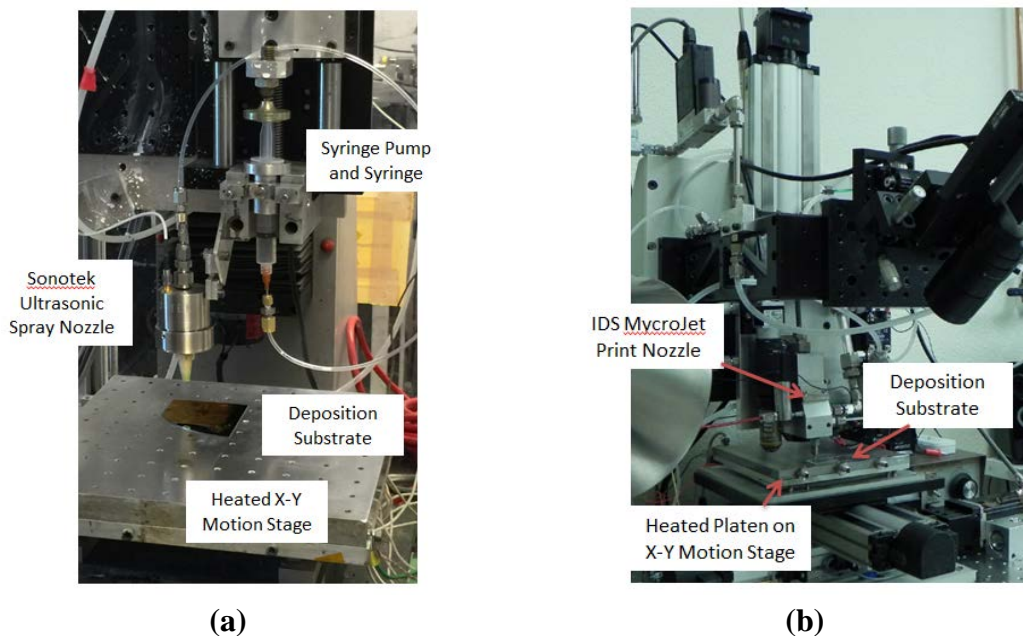


Figure 2. Experimental setup used for aerosol coating processes: (a) Sono-Tek ultrasonic spray nozzle used for depositing 30-40 μm droplets and (b) MycroJet print head used for depositing 0.5-3 μm droplets.

The second aerosol print technology used was an IDS MycroJet (MJ) print head which has an operating frequency of 2.8MHz and produces droplets ranging from 0.5 to 3 μm (See Fig.1b). The MJ print head aerosolizes liquid materials ranging from 1-20cP and has a self-contained reservoir where the liquid is aerosolized before printing. The aerosol is transported to the print head using a carrier gas. In the print head, a second gas stream is introduced coaxially to the aerosol gas stream to collimate and accelerate the aerosol droplets to be impacted onto substrate surface. The output rate of the aerosol is kept constant by controlling the aerosol carrier gas flow rate and the temperature of the atomization chamber. A heated platen is used to control the substrate temperature to affect the rate of solvent evaporation from the aerosol droplets and the printed polyimide film. The platen is attached to the CNC motion platform to print the film using specific motion pattern. The printed linewidth from the MycroJet print head ranges from approximately 10 μm to 0.5 mm. The output rate from the MycroJet print head can be varied from 0.1-10 mL/hr. The focus of the MJ printing was to demonstrate feasibility of this technology to print PI films/features.

Two polyimide solutions were used for the printed film testing. The first material is a polyamic acid solution (Sigma-Aldrich 575828) 15wt% in NMP/aromatic hydrocarbons (SAPI). The second material is a proprietary formulation of a polyimide precursor in ethanol (UT Dots PI1-AJ) (UTDPI in this paper). Both the SAPI and UTDPI solutions were deposited using the STA nozzle while only the UTDPI solution was deposited using the MJ print head.

All polyimide samples were deposited on Au coated Si wafers which were air plasma cleaned immediately prior to polymer deposition. The polymer solution was degassed at 60 $^{\circ}\text{C}$ in a vacuum oven prior to deposition and the material dispensed as dictated by the program/toolpath. On completion of the deposition the material is thermally treated to evaporate solvent and for polyamic acid to polyimide conversion. The STA nozzle was set to an operating voltage of 7.5V for all depositions. The polymer solution was loaded into a syringe and degassed as described above. For spray deposition the SAPI solution had to be further diluted with NMP (1:8 v/v). The spray nozzle was positioned approximately 1 inch above the substrate with sheath gas flow rate of 4 lpm. The platen was heated to 80 to 120 $^{\circ}\text{C}$ and the material dispensed as dictated by the program/toolpath.

The toolpath used in this work is shown in Figure 3. The travel speed for the spray process was 900 mm/min. The printed area was 55 mm square and a serpentine pattern was used to cover the spray area uniformly. For each subsequent print layer, the serpentine pattern was rotate by 90 $^{\circ}$. The pitch between adjacent lines is 2.5 mm and a single print layer consisted of two orthogonal serpentine print patterns. Before beginning testing, the solution output rate was adjusted to provide a spray on the Au wafer surface with sufficient viscosity to avoid puddling and flowing after printing. A solution output rate of 0.3 mL/mm of print distance was settled upon for all testing. All samples were print with the STA nozzle were printed with this output rate.

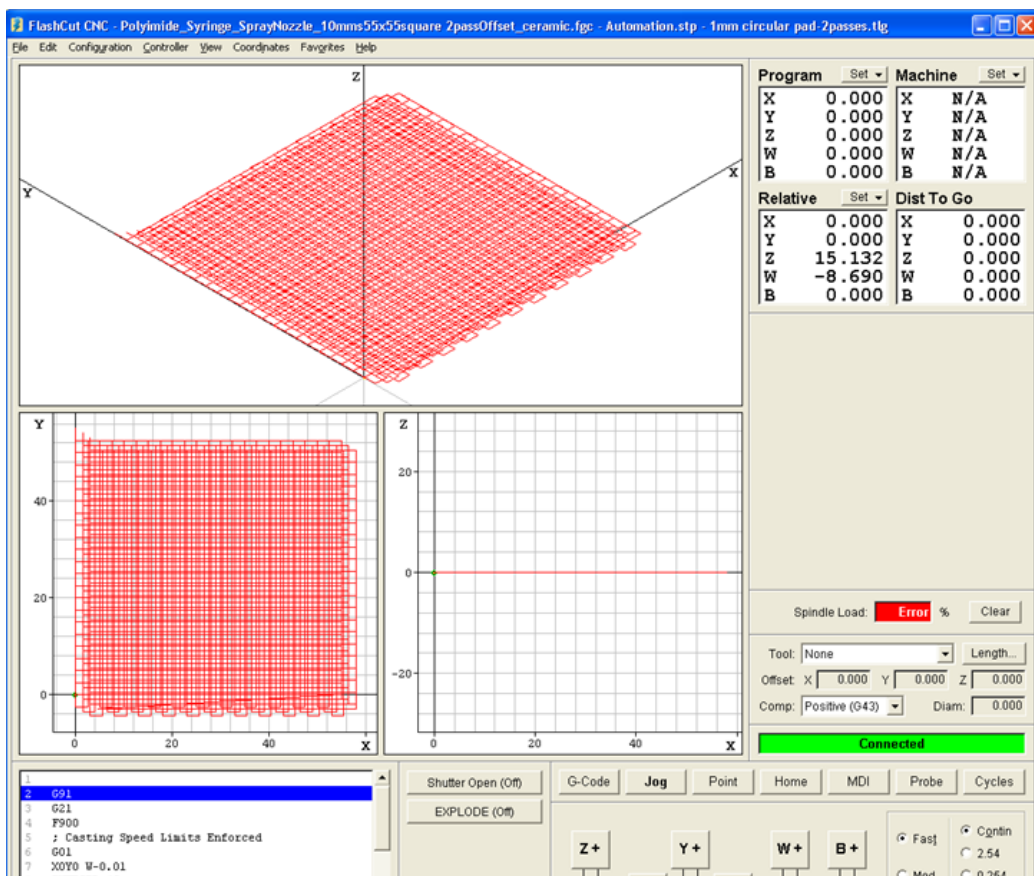


Figure 3. Screen shot of FlashCut front end showing pattern used for printing of PI films.

The toolpath developed for showing feasibility of using the MJ process to also create PI films are given in Table 1. The toolpath used consisted of a serpentine pattern with a pitch between adjacent lines of approximately 100 μm .

Post deposition heat treatment of the SAPI samples was performed at 215 $^{\circ}\text{C}$ for >12 hours. The UTDPI samples were sprayed using the STA nozzle without dilution and then cured at 300 $^{\circ}\text{C}$ for >12 hours. For some samples, a 2-3 hour lower temperature phase (90-130 $^{\circ}\text{C}$) was added prior to the final cure to mitigate film cracking or bubbling due to rapid solvent evaporation. No significant differences in dielectric performance were observed in the samples studied based on cure profiles.

After curing samples are metallized on the top surface with an array of 6.3mm diameter Au electrodes (50 nm Au). Commercial polyimide films are metallized with the electrode array (top) and a blanket Au metallization (50 nm) on the back to mimic the electrode geometry of the samples deposited on the Au/Si wafers. Each film sample accommodated between 20-30 test electrodes per sample.

Table 1. Process conditions used for MJ printing of UTDPI films.

Aerosol flow rate (ccm)	20
Sheath flow rate (ccm)	45
Print speed (mm/s)	5
Substrate temperature (deg. C)	60
Number of passes	8-16

Results & Discussion

Figure 4 shows a series of Si wafers with Au coated electrodes that were spray coated with the STA spray nozzle using the UTDPI polyimide solution. These results are typical for both the STA spray process using UTDPI and SAPI polyimide solutions. While these wafers were being coated with the UTDPI solution, the substrate temperature varied between 80°C and 120°C to characterize the effect of substrate temperature on printed film quality. These wafers were coated with a single layer of the UTDPI (2 orthogonal serpentine patterns) as previously described.

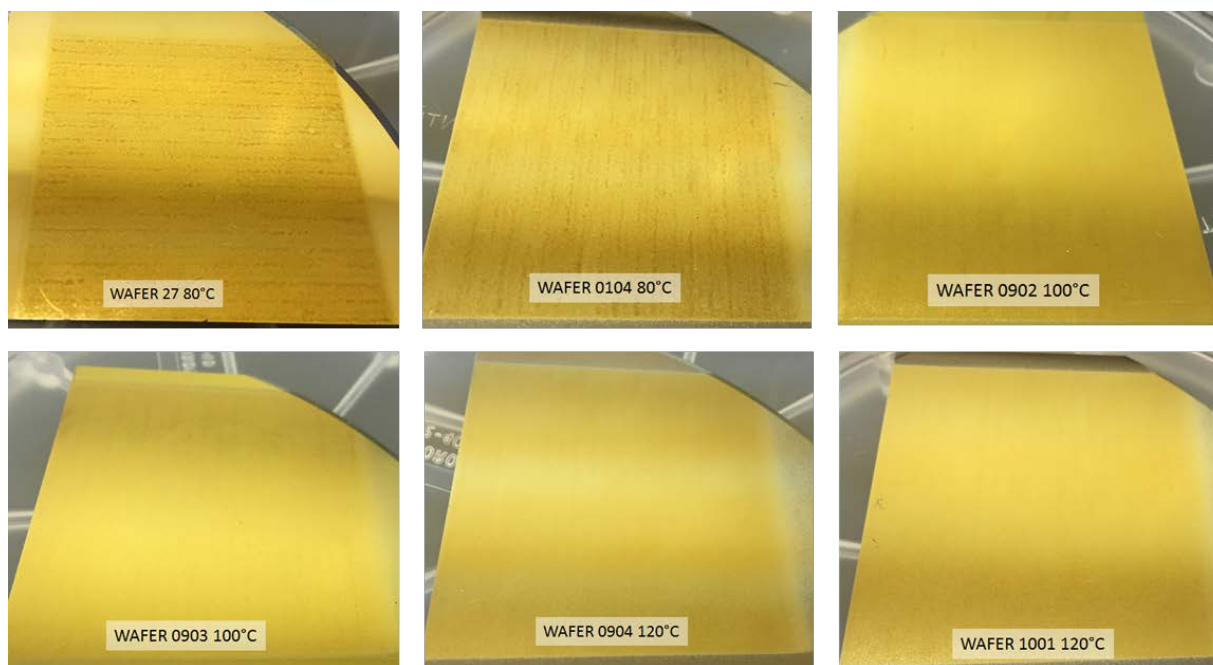


Figure 4. Series of Si wafers with AU electrodes spray coated with UTDPI solution while substrate temperature was varied from 80°C to 120°C.

Table 2 shows film thickness and surface roughness measurements for the STA spray coated wafers shown in Figure 4. These results show a decrease in average film thickness as the substrate temperature is increased. In addition, the Maximum Peak Height and Peak to Valley Difference decrease by almost 20% as the substrate temperature is varied from 80°C to 120°C. Finally, it is important to notice that the Valley Depth from Mean is less than 1 μm for all of the sprayed films. This small difference between the average film thickness and the valley depth from mean would suggest that most of the sprayed film has a thickness near the average film thickness plus/minus the valley depth from mean and that the very large difference in the maximum peak height is a result of a relatively small number of surface defects.

Table 2. Spray deposited polyimide film thickness and surface roughness measurements taken for samples shown in Figure 4.

	Average Thickness (μm)	Max. Peak Height (μm)	RMS Roughness (μm)	Peak to Valley Difference (μm)	Valley Depth from Mean (μm)
W27-80C	6.45	51.86	2.3	50.90	0.96
W104 80C	6.25	54.40	1.86	53.42	0.98
W0903 100C	5.56	48.1	2.31	47.15	0.94
W0903 110C	5.30	50.47	2.41	49.55	0.92
W0904 120C	4.60	32.16	2.18	31.21	0.95
W1001 120C	4.99	43.02	2.35	42.10	0.91

The concept that (1) the sprayed film has a thickness near the average film thickness plus/minus the valley depth from mean and (2) that the very large difference in the maximum peak height is a result of a relatively small number of surface defects is supported by the optical profilometry images and SEM images of the spray formed UTDPI films shown in Figure 5 and Figure 6, respectively. The optical profilometry image shown in Figure 5 shows that there are only a limited number of points with a very large thickness difference than the parent film. The scanning electron microscope image of the UTDPI film cross-section shows very clearly that there are a small number of relatively large particles on the surface of the film. It will be important with future work to understand how to minimize the formation of the particles and also to understand the impact of these particles on the electrical performance of the printed capacitors.

Dielectric permittivity, dielectric loss and dielectric strength testing were performed on a series of capacitors fabricated using varying dielectric films including the STA spray coated films(4). The results of these measurements are shown in Table 3 and Table 4. As can be seen from the results in Table 3 and Table 4, the spray coated dielectric films have higher dielectric loss than the commercial film. Also, the dielectric breakdown strength for the STA nozzle sprayed UTDPI is approximately half that of the commercial film whereas the STA nozzle sprayed SAPI film has a dielectric breakdown strength that is less than 25% of dielectric breakdown strength of the commercial film.

Surface Stats:

Ra: 2.01 μm

Rq: 2.35 μm

Rt: 45.01 μm

Measurement Info:

Magnification: 2.51

Measurement Mode: VSI Film

Sampling: 3.95 μm

Array Size: 640 X 480

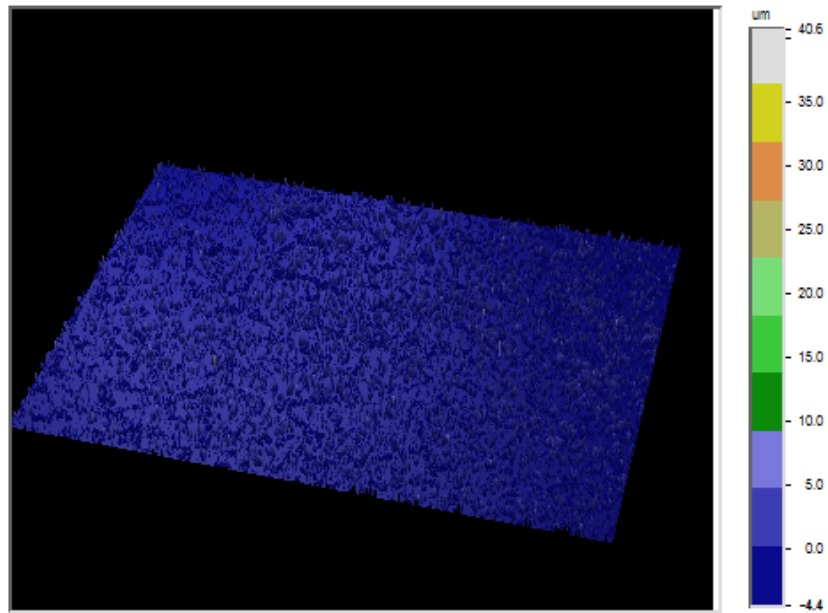


Figure 5. 3D surface plot of UTDPI spray coated film deposited using the STA spray nozzle. Image taken using Wyko optical profilometer.

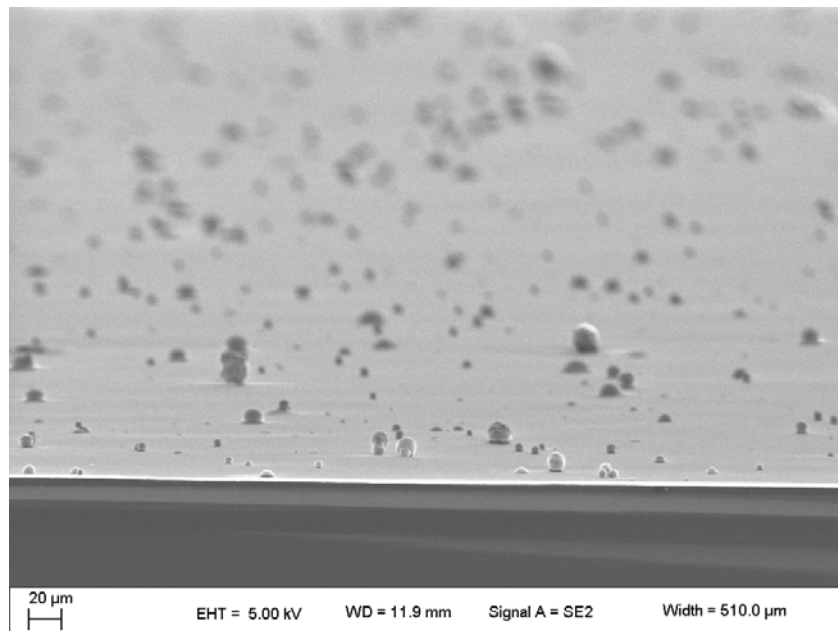


Figure 6. Cross-sectional view of STA spray UTDPI sample, showing surface roughness and overspray of polymer on the film surface.

Figure 7 and Figure 8 show results of feasibility work performed on MJ printing platform. Figure 7a shows the MJ printing process depositing UTDPI film. Figure 7b shows two printed UTDPI pads on Au coated wafer. Figure 8a shows the same MJ printed UTDPI pads with a MJ printed Au pad on top of the dielectric pad. Figure 8b shows thickness measurements for the MJ printed capacitor shown in Figure 8a. The capacitance value for the capacitor shown in Figure 8a was between 100-200pF.

Table 3. Permittivity and Dielectric Loss Mean (St. Dev)

Group	N*	N _{ex} *	Avg. thickness (μm)	κ	Df
AM spray SA PI	38	6	9.7 (2.5)	3.25 (0.63)	0.0058 (0.0141)
AM spray UTD PI	83	2	6.6 (1.8)	3.05 (0.77)	0.0021 (0.0005)
AM syringe SA PI	97	2	37.3 (14.7)	3.94 (1.26)	0.0080 (0.0058)
Commercial	90	0	13.3 (0.2)	3.25 (0.02)	0.0021 (0.0004)
Solvent cast SA PI	104	0	16.1 (6.2)	3.64 (0.47)	0.0020 (0.0005)
Solvent cast UTD PI	42	11	2.6 (0.9)	3.25 (0.64)	0.0036 (0.0005)

* N is the total number of electrodes measured. N_{ex} is the number of electrodes either not measured or excluded after measurement (as described in methods section). N + N_{ex} is the total number of test electrodes fabricated for each group.

Table 4. Dielectric breakdown strength

Group	N	Weibull α (kV/cm)	Weibull β
AM spray SA PI	47	1110	0.8
Solvent cast UTD PI	54	2060	1.0
AM spray UTD PI	69	2402	1.5
AM syringe SA PI	101	3835	2.1
Solvent cast SA PI	103	4072	3.8
Commercial	89	4891	13.0

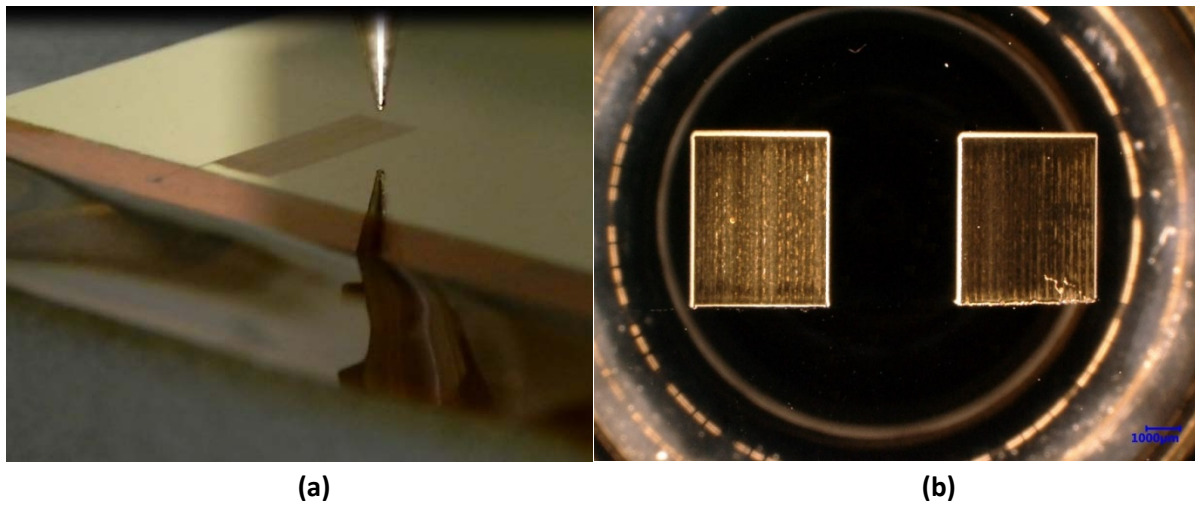


Figure 7. Photographs showing (a) MJ printing of UTDPI dielectric film and (b) printed UTDPI films on Au coated Si wafer.

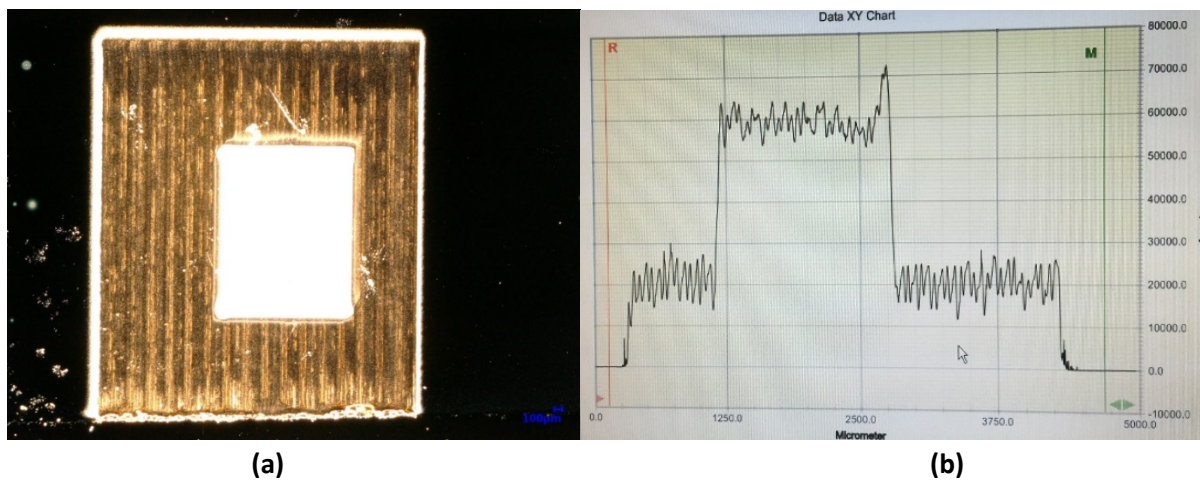


Figure 8. Photographs showing (a) MJ printed Au pad on printed UTDPI dielectric film forming capacitor and (b) profilometry data for printed capacitor shown in (a).

Conclusions

Two methods have been demonstrated to print polyimide films for capacitors. Both methods should be capable of printing capacitors onto non-planar surfaces with uniform coating thickness. Although the electrical breakdown strength of the spray coated polyimide films is much less than that of a commercial film, the current breakdown strength is very good given the

maturity of the printing processes. Focus on improving surface roughness of the printed films should provide improvements in the printed film quality and performance.

References

1. Jia Zhou, Tong Ge, Eileen Ng, and Joseph S. Chang, “Fully Additive Low-Cost Printed Electronics With Very Low Process Variations”, IEEE Transactions on Electron Devices, Vol. 63, No. 2, Feb. 2016, 793-799.
2. Rogers, J. A. (2010). Electronics: A diverse printed future. *Nature*, 468(7321), 177-178. doi:10.1038/468177a.
3. Lewis, J. A., & Ahn, B. Y. (2015). Device fabrication: Three-dimensional printed electronics. *Nature*, 518(7537), 42-43. doi:10.1038/518042a.
4. Yong-Young Noh¹, Yong Xu¹, Mario Caironi² and Thomas D Anthopoulos³,”Preface: Printed electronics, *Semiconductor Science and Technology*, Volume 30, Number 10, Sept. 2015.
5. S. E. Berberich, A. J. Bauer and H. Ryssel, “High Voltage 3D-Capacitor”, 2007 European Conference on Power Electronics and Applications, Sept. 2007, pp1-9.
6. M. Detalle, M. Barrenetxea, P. Muller, G. Potoms, A. Phommahaxay, P. Soussan, K. Vaesen, W. De Raedt, “High density, low leakage Back-End 3D capacitors for mixed signals applications”, *Microelectronic Engineering* 87 (2010) 2571–2576.
7. P. Sarbol, A. Cook, P.G. Clem, D. Keicher, D. Hirschfeld, A.C. Hall, N.S. Bell “Additive Manufacturing of Hybrid Circuits” *Annu. Rev. Mater. Res.* Vol.46, 2016 in press.
8. L.N. Appelhans*, D. M. Keicher, J.M. Lavin, “Comparison of Dielectric Properties of Additively Manufactured vs. Solvent Cast Polyimide Dielectrics”, *CEIDP Proceedings*, 2016 in press.

Acknowledgements

Thank you to the following people for assistance and input in this work: Zach Beller, Seth Johansen.

Sandia National Laboratories is a multi-program laboratory managed and operated by Sandia Corporation, a wholly owned subsidiary of Lockheed Martin Corporation, for the U.S. Department of Energy’s National Nuclear Security Administration under contract DE-AC04-94AL85000.